

BEAM TRANSPORT CALCULATION FOR K-500 CYCLOTRON OPERATION AT MICHIGAN STATE UNIVERSITY

J. Kasagi, S. Angius and E. Kashy
Cyclotron Laboratory, Michigan State University
East Lansing, MI 48824

Summary

The design of the beam transport and analysis system for the experimental facility using the K-500 superconducting cyclotron at M.S.U. and which is currently being assembled is described.

Introduction

The beam transport calculation for the experimental facility using the K-500 superconducting cyclotron has been carried out by using various beams expected from the K-500 cyclotron. The final design of the beam transport and analysis system has been made from these calculations. The system not only can deliver any kind of beams from the K-500 cyclotron to the experimental area but also can provide for a variable linear dispersion at the target positions of the magnetic spectrographs. This paper describes the beam transport system which is currently being assembled.

Experimental Floor Plan for K-500 Cyclotron

The layout of the experimental floor with beam transport element is shown in Fig. 1. The experimental area is separated into two large rooms designated North and South. The South vault houses a 60 inch scattering chamber, a prototype version of the reaction product mass separator, a gamma ray goniometer and target chamber for the cryogenic helium-jet apparatus. The North vault houses the Enge split pole spectrograph, the S320 spectrograph with a K=320 bending capacity, a scattering chamber planned for neutron experiment and a low rigidity (K=250) beam line. The S320 spectrograph is also used as a portion of the beam transport elements for the Enge split pole beam line and for the neutron chamber beam line as shown in Fig. 1.

The first section of the transport is the region from the exit of the K-500 cyclotron to the first slit position (S1). There are 6 quadrupole magnets and one small dipole magnet in this section. The beam is bent by the dipole magnet located after the S1 and distributed to each target positions by the next dipole magnet.

Beam Transport from the Cyclotron to the Initial Waist

The properties of the beams from the K500 cyclotron were calculated by ray-tracing method.¹ In this calculation, the effect of the magnetic channels of the extraction system were included using the result of the magnetic field measurement. Eight different beams which correspond to the extreme conditions of the cyclotron were provided for the transport calculation. Table 1 shows the calculated beam properties at cyclotron exit for several beams. They are very different from each other. An unusual feature of the extraction system of the K500 cyclotron, which consists entirely of inert focusing elements, strongly influences the beam properties. This feature greatly simplifies design and construction of the extraction system itself but at the cost of a variability in direction and focusing conditions for beams leaving the cyclotron. The first section of the transport system must then be used as an active element to compensate for this variability in order to bring all beams to an approximately identical phase space condition at the location of S1.

The arrangement of the transport elements was carried out by using the code TRANSPORT.² The six quadrupole magnets located in this section are found to be a sufficient number of optical elements to control any beam from K-500 cyclotron to the S1 position. The resulting properties of beam 1, 5, 6 and 7 at the S1 are almost same as shown in Table 2. Figure 2 shows an example of the beam envelope of two extreme beams tracked through this section of the optical system.

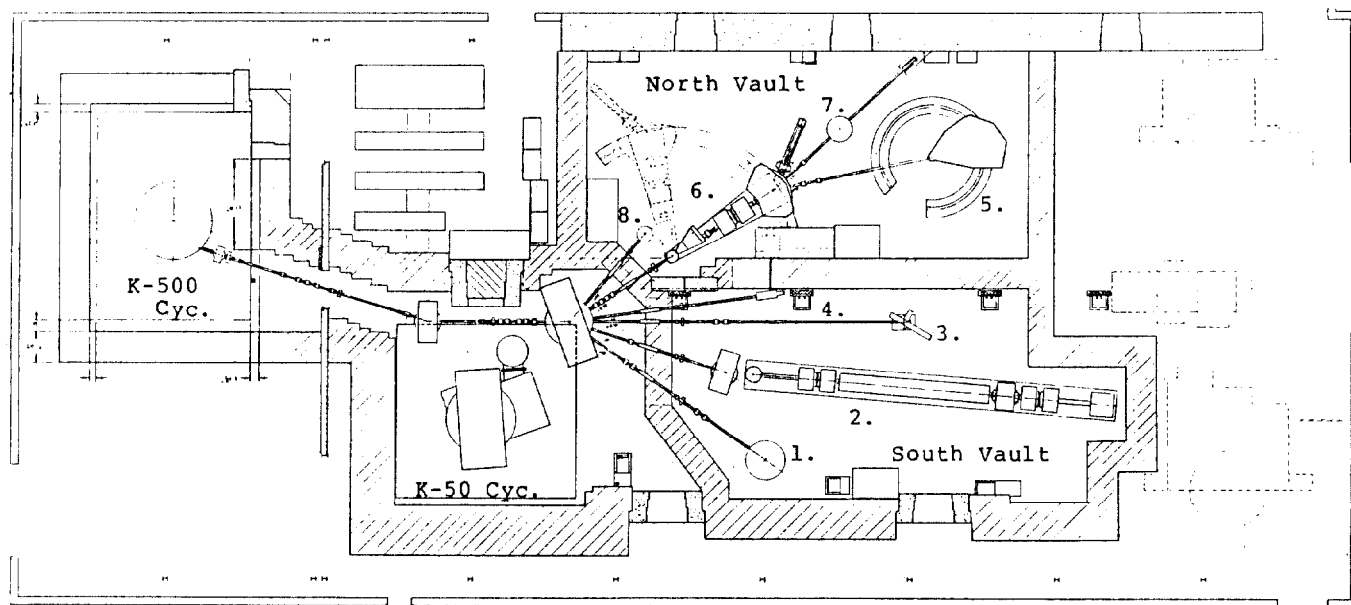


FIG. 1. Layout of the experimental floor. 1. 60 inch Scattering Chamber. 2. Recoil Product Mass Separator. 3. γ -ray Goniometer. 4. Cryogenic He Jet. 5. Enge Split-pole Spectrograph. 6. S320 Spectrograph. 7. Neutron Scattering Chamber. 8. K=250 beam line.

Table 1. Characteristics of several beams at Cyclotron exit.

Beam #	#1	#5	#6	#7
Charge State (Q/A)	0.02	0.322	0.332	0.5
Energy (MeV/A)	0.206	49.87	22.20	59.72
Horizontal size, x(cm)	0.46	0.49	0.34	0.235
Horizontal divergence, θ (mrad)	1.63	0.85	0.89	1.25
r_{12}^*	-0.917	-0.725	0.591	0.694
Vertical size, y(cm)	0.245	0.12	0.36	0.215
Vertical divergence, ϕ (mrad)	4.25	3.25	2.50	1.20
r_{34}^*	0.977	0.639	0.861	0.553
Dispersion, R_{16} (cm/% $\Delta P/P$)	-14.36	-18.12	-0.96	-4.89
Angular Dispersion, R_{26} (mrad/% $\Delta P/P$)	23.66	15.04	21.37	13.40

*) Matrix element of the beam matrix used in TRANSPORT.²

Table 2. Beam characteristics at the first waist (S1). The notations are same as Table 1.

Beam #	x(cm)	θ (mrad)	y(cm)	ϕ (mrad)	R_{16}	R_{26}
1	0.13	2.35	0.04	5.91	5.77	-20.1
5	0.20	1.41	0.08	3.77	7.32	-22.2
6	0.16	1.54	0.10	4.61	4.78	-16.3
7	0.11	1.89	0.07	3.12	4.50	10.8

Beam Transport to the Target Positions

The transport system from the S1 position to each target position is designed using beams 5 and 6. The following conditions as well as the beam size at each target position were checked to determine the final arrangement of the transport elements. They are the maximum beam size for each beam line (less than 3 cm), the maximum field gradient of the quadrupole magnet which is limited by power supply and the total current of all the quadrupole magnets. Furthermore, for the S320 spectrograph and for the Enge split pole spectrograph, the system was required to provide for a variable linear dispersion at the target positions so

Table 3. Beam parameters at the target locations for various beam lines (Beam 6).

	x(cm)	θ (mr)	y(cm)	ϕ (mr)	R_{16} (cm/%)	R_{26} (mr/%)
Low rigidity	0.43	3.38	0.45	4.77		
S320	0.04	6.72	0.13	3.54	-2.19	67.54
Split pole	0.06	4.30	0.17	2.78	4.58	-43.17
Neutron Chamber	0.06	3.93	0.12	3.69		
He jet	0.22	1.20	0.42	1.18		
γ -ray	0.09	2.85	0.22	2.11		
RPMS	0.34	1.00	0.07	6.75		
Scatt. Chamber	0.12	1.99	0.22	2.08		

that matching conditions in the "energy-loss" mode can be achieved for a wide variety of reactions. The final arrangement of the transport elements is shown in Fig. 1. Figure 3 shows an example of the beam envelope of #6 beam for Enge Split-pole line. The beam properties at various target positions calculated for beam 6 are summarized in Table 3. Very similar properties can be realized for beam 5. Therefore, the designed system is expected to transport the various beams to any target positions as well as provide the desired linear dispersion matching conditions for both spectrographs.

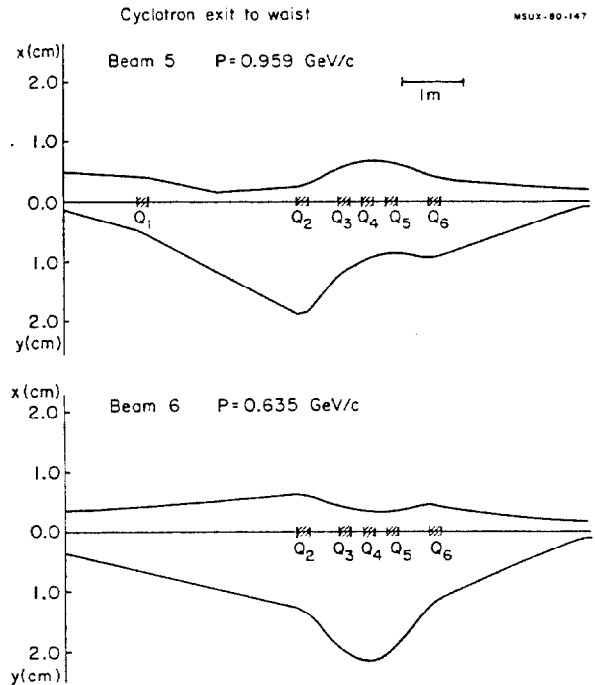


FIG. 2. Plot of horizontal and vertical beam envelopes from cyclotron exit to the waist located at the first defining slit. The two beams represent the extreme limits of the distribution of focusing conditions for beams leaving the cyclotron.

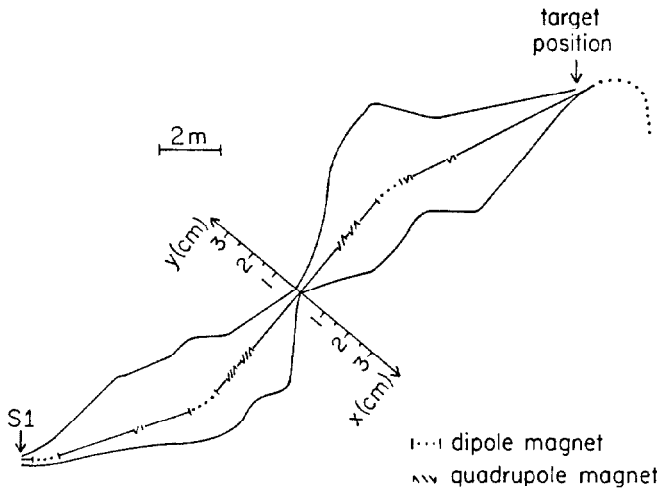


FIG. 3. Plot of beam envelopes from the first waist position to the target position of Enge Split-pole Spectrograph. The scales of the vertical (y) and horizontal (x) sizes are perpendicular to the beam line.

References

1. E. Fabrici, D. Johnson and F. Resmini, To be published in Nucl. Inst. and Meth.
2. K.L. Brown, D.C. Carey, Ch. Cselin and F. Rothacker, Cern Report 72-16.